Author Manuscript

Author Manuscript

Author Manuscript

Author Manuscript

HHS Public Access

Author manuscript

J Mol Cell Cardiol. Author manuscript; available in PMC 2016 November 01.

Published in final edited form as:

J Mol Cell Cardiol. 2015 November ; 88: 91–100. doi:10.1016/j.yjmcc.2015.09.007.

An In Vitro Model for the Assessment of Stem Cell Fate Following Implantation within the Infarct Microenvironment Identifies ISL-1 Expression as the Strongest Predictor of c-Kit+ Cardiac Progenitor Cells' Therapeutic Potential

Kelly E. Sullivan[1], **Laura J. Burns**[1], and **Lauren D. Black III**[1,2,†]

[1]Department of Biomedical Engineering, Tufts University, Medford, MA, 02155, USA

[2]Cellular, Molecular, and Developmental Biology Program, Sackler School for Graduate Biomedical Sciences, Tufts University School of Medicine, Boston, MA 02111, USA

Abstract

Cell therapy has the potential to drastically improve clinical outcomes for the 1.45 million patients suffering from a myocardial infarction (MI) each year in the U.S. However, the limitations associated with this treatment -including poor engraftment, significant cell death and poor differentiation potential - have prevented its widespread application clinically. To optimize functional improvements provided by transplanted cells, there is a need to develop methods that increase cellular retention and viability, while supporting differentiation and promoting paracrine signaling. Current *in vivo* models are expensive, difficult to access and manipulate and are time consuming. We have developed an *in vitro* model of MI which allows for a straightforward, consistent and relatively accurate prediction of cell fate following injection *in vivo*. The model demonstrated how the infarct environment impairs cellular engraftment and differentiation, but identified an implantation strategy which enhanced cell fate *in vitro*. Multivariate linear regression identified variables within the model that regulated vascular differentiation potential including oxygen tension, stiffness and cytokine presence, while cardiac differentiation was more accurately predicted by Isl-1 expression in the original cell isolate than any other variable present within the model system. The model highlighted how the cells' sensitivity to the infarct variables varied from line to line, which emphasizes the importance of the model system for the prediction of cell fate on a patient specific basis. Further development of this model system could help predict the clinical efficacy of cardiac progenitor cell therapy at the patient level as well as identify the optimal strategy for cell delivery.

[†]**Correspondence should be addressed to**: Lauren D. Black (lauren.black@tufts.edu), Department of Biomedical Engineering, Tufts University, 4 Colby Street, Medford, MA 02155, Fax: 617-627-3231, Phone: 617-627-4660.

Publisher's Disclaimer: This is a PDF file of an unedited manuscript that has been accepted for publication. As a service to our customers we are providing this early version of the manuscript. The manuscript will undergo copyediting, typesetting, and review of the resulting proof before it is published in its final citable form. Please note that during the production process errors may be discovered which could affect the content, and all legal disclaimers that apply to the journal pertain.

Disclosures: None

Author Manuscript Author Manuscript Author Manuscript Author Manuscript

Keywords

Stem cell-microenvironment interactions; Myocardial infarction; c-Kit+ cardiac progenitor cells; in vitro disease modeling

Introduction

Stem cell therapy for the treatment and prevention of heart failure (HF) following myocardial infarction (MI) has the potential to benefit over 5 million people in the U.S alone [1]. Although cardiac progenitor cells (CPCs) contribute to a limited or negligible population of cardiomyocytes (~0.03%) in the adult heart throughout physiological development [2], neonatal hearts demonstrate the ability to regenerate cardiac muscle following myocardial injury through CPC mediated myogenesis [3]. Despite their limited ability to regenerate myocardium in the adult heart, c-Kit+ CPCs have a high propensity for vascular differentiation and contribute to approximately 3% of all CD31+ endothelial cells within native myocardium and 7% in the injured heart [2]. The intramyocardial delivery of these cells for the treatment of MI has demonstrated clinical efficacy in two human Phase I trials, CADUCEUS and SCIPIO [4]. In the CADUCEUS trial, six months following cell therapy treatment, cardiosphere-derived autologous stem cells demonstrated regenerative potential. Patients receiving cells possessed smaller infarct scars and more viable tissue mass. Despite the minimal cardiomyogenic potential of these cells, research has demonstrated their potential to promote angiogenesis and decrease cellular apoptosis and necrosis following injury *in vivo*, either through their differentiation towards vascular lineages [5] or via secretion of growth factors [6] and/or extracellular miRNAs [7]. However, poor engraftment and viability minimizes the percentage of injected cells that contribute to functional improvements and enhanced cardiac outcomes [8].

The development of implantation strategies, which either focus on pre-conditioning the cells prior to injection or delivering the cells in conjunction with a small molecule, growth factor or other cell type, have demonstrated significant benefit as compared to the delivery of CPCs alone. However, identifying the specific mechanisms responsible for either the therapeutic efficacy of the cells or the implantation strategy is challenging within the complex infarct microenvironment. In addition, the variability in the remodeling process following myocardial injury [9] and the heterogeneity of patient derived CPCs [10] makes it challenging to predict the most beneficial delivery strategy for an individual patient. While most animal studies demonstrate the efficacy of a singular implantation strategy, it remains to be seen whether a specific approach is most effective or whether the effectiveness is specific to a particular animal's infarct microenvironment and/or population of CPCs. To address the current limitations of cell therapy treatment of MI, it is critical to develop an *in vitro* model system which will possess the predictive capacity at the patient-specific level to determine the most effective approach to regenerate necrotic myocardium via stem cell therapy. The ideal model would not only be easy to access and manipulate, but also possess the capacity for high-throughput analysis.

Author Manuscript Author Manuscript Author Manuscript Author Manuscript

Several signaling moieties within the extracellular environment impact CPC fate including, but not limited to, extracellular matrix composition [11], substrate stiffness [12], oxygen tension [13], soluble growth factors [14] and inflammatory mediators [15]. These factors change significantly within the infarct microenvironment in response to coronary artery occlusion and in conjunction with a massive inflammatory response. Previous work in our lab has demonstrated that the altered matrix composition of the infarcted myocardium promotes pro-survival paracrine signaling between mesenchymal stem cells (MSCs) and oxidatively stressed cardiomyocytes *in vitro* [16], while the vascular differentiation potential of c-kit+ CPCs is enhanced in fibrin hydrogels of increased stiffness containing cardiac ECM derived from adult hearts but not in gels containing neonatal cardiac ECM [12]. However, understanding how both oxygen tension and immunomodulatory cytokines influence cellular engraftment, viability, differentiation potential and paracrine signaling within the context of the remodeled extracellular matrix is critical for an accurate prediction of cell fate *in vivo*. The incorporation of decellularized extracellular matrix isolated from both healthy and infarcted rat hearts into a polyacrylamide gel system allowed for the development of a complex model descriptive of the infarct microenvironment with the application of hypoxic cell culture and inclusion of soluble, inflammatory mediators. This model system was used to not only predict the regenerative potential of c-kit+ CPCs isolated from individual infarcted rat hearts, but also assess the efficacy of an implantation strategy. Further development with this *in vitro* model system could help predict the ideal approach for cell therapy on a subject specific basis with direct, clinical applications.

Materials and Methods

Rodent model of MI

Animal experiments were approved by the Institutional Animal Care and Use Committee at Tufts University and performed in agreement with Tufts University guidelines and the US Animal Welfare Act. MI was induced in male Sprague-Dawley rats (2+ months of age and 250–275 grams). Following induction of anesthesia with isoflurane, an incision was made between the fourth and fifth intercostal space. The heart was exposed and a 6-0 prolene suture was used to permanently occlude the coronary artery. Location of ligation was chosen such that blanching occurred across 40–50% of the left ventricular free wall and a GE Vivid I ultrasound and a 12S-RS Phased Array Transducer (5.0 – 11.0 Mhz) were used to collect M-mode echocardiograms in order to ensure significant functional deterioration following MI. Animals recovered for either 1 or 4 weeks post-infarction depending on whether they were used for cell isolation or ECM, respectively.

c-Kit+ CPC isolation and characterization *in vitro*

1 week following MI, animals were sacrificed via CO_2 asphyxiation and whole hearts were isolated and immersed in ice cold PBS-glucose (Figure 2A). The whole organ was minced into 1 mm^3 pieces. A serial collagenase digestion protocol [17] was adapted to maintain cell viability during the isolation, but also to maximize cell retrieval from the tissue and is described in detail within the supplemental methods. The cell pellet was resuspended in 2mL of 1× insulin-tranferin-selenium (ITS), 1% Pen-Strep in Ham's F-12 Nutrient Mixture. c-kit+ CPCs were isolated according to a previous protocol [11]. Briefly, a rabbit polyclonal

Author Manuscript Author Manuscript Author Manuscript Author Manuscript

c-kit antibody (Santa-Cruz, H-300) was conjugated to magnetic beads, added to the cells and incubated for 2 hours at 37 °C on an end-over-end rotator. The c-kit+ CPCs were isolated via magnetic assisted cell sorting and maintained in F-12 supplemented with 10% FBS, 1% Pen-Strep, with 10 ng/ml FGF-2 (R&D, 234-FSE-025) and 10 ng/mL LIF (R&D, 7734-LF-025) added fresh at each feeding.

6 different lines of c-kit+ CPCs were isolated and characterized via qPCR and histological assessment at passages 2 and 3. Spontaneous differentiation was also assessed by removing the cells from their maintenance media and placing them in a serum-free media, which consisted of a 1:1 mixture of Ham's F-12 and DMEM with a 0.2% (w/v) bovine serum albumin, 0.5% ITS and 1% Pen-Strep. Following 1 week in culture, differentiation was assessed via qPCR and histological assessment at passages 5 and 6. Cells were frozen in liquid nitrogen at passage 3. Cells were thawed and cultured for 2 passages prior to seeding in the model system.

Model development and application for the prediction of cell fate

MI Model: Cell and ECM Isolations—Hearts were isolated from healthy animals or 4 weeks post-infarction and subjected to retrograde perfusion decellularization with 1% sodium dodecyl sulfate (SDS). Tissue isolated from either the free wall of the left ventricle of healthy hearts or from the scar region of infarcted hearts was lyophilized and solubilized as described previously [18] in a 1mg/ml solution of Pepsin in 0.1M HCl for 48 hours to reach a final solubilized ECM concentration of 5mg/ml.

Model System Development—Parameters (including stiffness, composition, oxygen tension and cytokine presence) recapitulated within the model system were selected based on previous characterization of both native and infarct extracellular environments *in vivo*. More specifically, the increase in myocardial stiffness following infarction from 18±2 kPa to 55±15 kPa measured in a rat model of MI [19] was modeled via a polyacrylamide gel platform in which.gels were fabricated at approximately 25±6 kPa and 48±7 kPa by altering the cross-linking between acrylamide and bis acrylamide. Alterations to the extracellular matrix composition following infarction has been previously characterized [16] and to model these compositional changes *in vitro* 400 μg of healthy ECM was cross linked into 500uL of PA gel solution of 25 kPa stiffness, while 400 μg of 4 week infarct ECM was cross linked into 40 kPa gel solution using acrylic acid-Nhydroxysuccinimide (NHS) ester to create covalent linkages between amine groups. 30uL of gel solution was cast onto an activated coverslip and a non-activated coverslip was placed on top to create an even surface and promote polymerization according to a previously published protocol [20]. After 30 minutes, gels were washed with sterile 1× PBS three times for 5 minutes.

Oxygen tension was also varied within the model system to specifically mimic the decrease in oxygen content from approximately 5% O2 to 1% O2 following coronary artery occlusion in mammals [21]. Therefore, following seeding of 100,000 c-Kit+ CPCs onto the gels in 3 mL of serum-free media (described above). Gels of lower stiffness [22], incorporated with healthy, cardiac ECM were cultured at 5% O_2 [21, 23], which is characteristic of a native myocardial environment. Gels of higher stiffness [19], with infarct ECM, were cultured at

Author Manuscript Author Manuscript Author Manuscript Author Manuscript

1% O_2 [21, 23] in a Biospherix C-Chamber with a ProOx P110 controller. To increase the complexity and validity of the model system, cytokines were included within the infarct model environment exclusively to mimic the inflammatory nature of the myocardial scar. However, due to the complexity of cytokines, growth factors and inflammatory mediators present within the myocardium following injury, we chose to exclusively model those factors which are in greatest abundance and have demonstrated the ability to regulate the CPC phenotype. Therefore, 5ng/mL bFGF [24] and 2.5 ng/mL TGF-β [25] were added to the culture media at the time of seeding to mimic the infarct microenvironment. The alterations in the extracellular environment modeled in this system are summarized in Figure1A and 1B.

Media was not changed during the 1 week culture period to more accurately model the native environment and minimize disruptions in oxygen tension. Cell adhesion and viability was assessed at both 16 hours and 5 days following seeding via a Live/Dead assay (Invitrogen). Cells were trypsinized with 0.5% trypsin on day 5 and RNA was isolated with the RNAeasy kit (74104, Qiagen, Valencia, CA). RNA was quantified, treated with DNAse (Applied Biosystems) and reverse transcribed with the High Capacity cDNA Reverse Transcription Kit (Applied Biosystems) in a thermocycler according to the manufacturer's specifications. qPCR was performed with Taqman primers (KIT, VEGF, HGF, ISL1, NKX2.5, GATA4, MEF2C, TBX5, TNNT2, GATA6, VWF, KDR, TAGLN, ITGA1, ITGA2, ITGB1) and Taqman Universal PCR Master Mix. Fold change expression was calculated using the ΔΔCt method. Histological assessment was performed on day 7. Primary antibodies for c-Kit (sc-H300, 1:200), Isl-1 (ab-20670, 1:200), Gata4 (sc-25310, 1:100), Tbx5 (sc-17866, 1:100), TnT (ab10214, 1:100), vWf (Sigma, F3520, 1:100), Flk-1 (sc-6251, 1:100), Gata6 (sc-6251, 1:200), and α-SMA (sc-32251, 1:200) were diluted in a 1% BSA solution. Secondary antibodies (Alexa Fluor 488-conjucated donkey anti-rabbit 715-545-152, Cy3-conjugated donkey anti-mouse 715-165-150, Jackson ImmunoResearch, West Grove, PA) were diluted at 1:400 in 1% BSA solution in PBS. Details regarding the histological staining protocol are further detailed within the supplemental methods. To better understand the alterations to cell fate as a function of the complex model environments, additional experiments were carried out to determine how each of the variables altered within the model environments independently regulated cellular adhesion, survival and differentiation potential. Alterations in cell adhesion and differentiation as a function of each individual variable including composition, stiffness, cytokine presence, and oxygen tension are summarized in supplemental figures 2, 3, 4 and 5, respectively.

The model studies were performed on three separate occasions. Each experiment used a unique cell line (2, 3 and 5) and ECM derived from different animals. Cardiac and vascular differentiation was assessed for all three lines (n=12/condition). Paracrine signaling was assessed for lines 3 and 5 (n=8/condition). Integrin signaling was assessed for Line 2 (n=4/condition).

Evaluation of implantation strategies

In order to assess an implantation strategy with the application of the model system, a TNFα receptor antagonist (sc-1070) [26] was delivered at 5μg/mL during the initial seeding and

Author Manuscript Author Manuscript Author Manuscript Author Manuscript

compared to cells seeded with no treatment. Cells were seeded at a higher density (300,000 cells/gel) because of the impaired attachment/proliferation within the infarct environment. A live/dead assay was performed and RNA isolated on day 5. Histological assessment was performed on day 7.

Multivariate Linear Regression Model

ΔCt values for gene expression were normalized from individual variable experiments (described in supplemental methods and data presented in supplemental figures 2, 3, 4 and 5) as well as all three model system studies. Independent variables were assigned normalized numerical values and are summarized in Table 1. Multivariate linear regression was performed for all three lines and adjusted R^2 values, coefficients and their respective p-values are reported in Table 2. Correlation coefficients were determined significant based on the null hypothesis that R=0. Significance was defined by α=0.05. For each gene of interest, the number of observations exceeded 90. When data from all three lines were compiled, the regression analysis for each gene of interest passed both the normality and covariance assumptions for all five genes. However, when the data was stratified based upon line (Table 3), the assumption of normality was not met for Line 2 and GATA4 expression and the constant variance assumption was not met for Line 2 and VWF.

Statistical Analysis

All results were analyzed with a student t-test or an appropriate sized multiple univariate analysis of variance with Student t-test post-hoc testing and corrected for multiple comparisons. P-values less than 0.05 were considered statistically significant.

Results

Significant heterogeneity exists across c-Kit+ CPCs isolated from infarcted rat hearts (Figure 2A). While cells were derived from the entire heart, separate isolations were performed on distinct regions of the heart and demonstrated that proliferative CPCs are primarily derived from atrial tissue at 1 week post-MI as compared to the infarct and remote ventricular tissue (data not shown). qPCR analysis of 6 cell lines demonstrates the variability which exists in stem, vascular and cardiac gene expression (Figure 2B). While lines 1, 2 and 3 express ISL-1 and, NKX2.5, lines 4, 5 and 6 did not express these same markers. Line 6 expressed the highest expression levels of intermediate and mature cardiac markers (TBX5, TNNT2). All six cell lines express similar levels of KIT following isolation. Histological staining of line 5 cells demonstrate robust expression of c-Kit, and minimal expression of Isl-1. The line appears more similar to a vascular progenitor with strong expression of Flk-1 and αSMA, but minimal expression of Tbx5 and TnT (Figure 2C).

CPCs were cultured for 1 week in serum-free media and no longer treated with LIF and bFGF (used to maintain stemness). As compared to stem maintenance media where more than 75% of the cells expressed c-Kit, in serum-free media, only 35% of the cells maintained c-Kit expression (Supplemental Figure 1C). The majority of the cells differentiated towards either a vascular or a cardiac phenotype. Gene expression levels of VWF doubled and

Author Manuscript Author Manuscript Author Manuscript Author Manuscript

almost 50% of the cells positively expressed this marker (Supplemental Figure1C and 1D). A proportion of cells possessed striated fibers stained positive for TnT. While spontaneous contractions were not observed, the increase in TNNT2 expression was robust and surpassed the levels of GAPDH.

Even though the model system was complex and recapitulated several components of the *in vivo* environment (Figure1A and 1B), it was easy to run multiple samples of different models in parallel. Each model was contained within a well of a 6 well plate and the ECM generated from a single heart was sufficient to develop 80 different model environments specific to the tissue source. In order to assess matrix and cell variability, the experiment was repeated on three separate occasions each time with a different line. Data collected from lines 2, 3 and 5 are described. Cells were capable of adhering and proliferating within each of the model systems despite the harsh culture conditions and lack of media change for 1 week in culture (Figure 3). However, stark differences in cell adhesion and proliferation existed across the two model systems and each line of c-Kit+ CPCs possessed a slightly variable ability to adhere and proliferate within the model environments. At 16 hours post-seeding, the healthy model system had a significantly greater number of cells per field than the infarct condition for both lines 2 and 3 ($p<0.001$). Over the next 4 days, the number of adherent cells increased approximately 3-fold in the healthy condition in lines 3 and 5 ($p<0.001$), while the density of cells within the infarct condition increased by only 2-fold ($p<0.05$). Line 2 cells remained relatively constant during the culture period, but all three lines possessed a significantly higher cell density in the healthy model than the infarct model at day 5 ($p<0.03$). Minimal differences in viability were detectable across conditions and this is likely due in part to the live/dead protocol, which requires rinsing of the gel prior to staining. Therefore, the majority of dead cells are removed prior to imaging and not quantified. In addition to adherence and proliferation, differentiation potential of c-Kit+ CPCs is significantly altered as a function of the infarct microenvironment (Figure 4). The infarct model increased expression of pro-survival (HGF) and pro-angiogenic (VEGF) cytokines (Figure 4C). While cardiac differentiation potential is consistent across the two populations, it is also minimal and suggests the native myocardial environment does not stimulate spontaneous cardiac differentiation. In contrast, the differentiation of c-Kit+ CPCs towards vascular lineages is significant with robust expression of αSMA and VWF within the healthy microenvironment (Figure 4A). However, the infarct microenvironment significantly abrogates the expression of vascular markers including TAGLN (SM22α) and VWF. Alterations in adhesion and differentiation may be a factor of integrin expression as ITGA2 expression is significantly increased within the infarct model system (Figure 4E).

An implantation strategy was assayed for its ability to enhance cell fate and treatment with a TNFα receptor antagonist did not significantly impact cell adhesion or viability (Figure 5A). Although c-Kit protein expression appears consistent with or without the implantation strategy (Figure 5B), ISL-1 expression was enhanced when the cells were delivered with the TNFα receptor antagonist (Figure 5C). While differentiation towards a vascular lineage was not affected (Figure 5D), the early cardiac transcription factor, GATA4, demonstrated increased expression in the presence of the TNFα receptor antagonist. However, TNNT2 expression was not altered (Figure 5E).

Author Manuscript Author Manuscript Author Manuscript Author Manuscript

Multiple linear regression analysis demonstrated that variation in cardiac differentiation potential is attributable to CPC line variability more significantly than any of the extracellular variables present within the infarct environment. In particular, the extent of ISL-1 expression in CPC isolates is the major determinant of both GATA4 and TNNT2 expression. TNNT2 expression was also positively regulated by increasing stiffness and negatively correlated with immunomodulatory cytokines (Supplemental Figure 3C and 4C, respectively and Table 2). Although TNNT2 and GATA4 expression levels were positively regulated by stiffness, sensitivities to cytokine presence and, most significantly, oxygen tension were line-dependent (Table 3). Only line 2 cells' expression of GATA4 and TNNT2 was positively regulated by oxygen tension and negatively impacted by cytokines (Table 3).

Vascular differentiation potential was influenced by the cell line and three of the four infarct variables. Similar to cardiac differentiation, collagen I density had a minimal, non-significant impact on VWF and TAGLN expression (Supplemental Figure 2D, Table 2). The degree of the association between ISL-1 and vascular gene expression was weaker as compared to the relationship with the cardiac differentiation markers. Stiffness and oxygen tension were both positively correlated with endothelial and smooth muscle cell differentiation (Supplemental Figures 3D and 5D, respectively and Table 2), while the presence of cytokines inhibited both markers' expression (Supplemental Figure 4D and Table 2). Lines 2 and 3 possessed very similar sensitivities to the infarct variables with respect to vascular differentiation, but line 2 was more responsive to oxygen tension with stronger correlations to both VWF and TAGLN gene expression, while line 3 cells demonstrated a more robust, negative correlation with cytokine presence (Table 3).

ISL-1 expression demonstrated the strongest, positive interaction with both stiffness and oxygen tension. ISL-1 expression was also positively correlated with the degree of ISL-1 expression in stem maintenance media and negatively correlated with cytokine presence (Table 2). While both lines 2 and 3 demonstrated similar interactions between ISl-1 expression and stiffness/cytokine presence, only line 2 possessed a strong, positive interaction between oxygen tension and ISL-1 expression (Table 3).

Discussion

The *in vitro* polyacrylamide gel based model system described herein demonstrates significant potential for the prediction of cell fate *in vivo* as it recapitulates four key aspects of the microenvironment which change following infarction including, increased substrate stiffness [27], altered matrix composition [28], decreased oxygen tension [23] and the presence of inflammatory mediators [29]. The application of the model system for the development of delivery strategies which maximize CPCs' therapeutic potential could increase the validity of cell therapy as a treatment option for the millions of people suffering from an MI each year. The *in vitro* platform is both easy to access and manipulate and has the potential to be scaled up due to its relative size and cost effectiveness, which allows for a comparative assessment of various implantation strategies as well as an evaluation of the heterogeneity which exists across patient populations. Ultimately, the model system has the potential to minimize the time, cost and variability associated with animal model studies by serving as a preliminary screen for the comparison of multiple strategies' effectiveness

Author Manuscript Author Manuscript Author Manuscript Author Manuscript

simultaneously as well as an identification of the underlying mechanisms responsible for enhanced cell fate.

The inability of CPCs to adhere and proliferate within the infarct environment demonstrates that the model system presents an inhospitable environment similar to the scar *in vivo* where it has been reported that fewer than 5% of injected cells are retained [8]. Assessment of the individual variables suggests that both oxygen tension and substrate composition are the two most limiting factors to CPC adhesion and expansion within the infarct model system. While short-term exposure to oxidative stress (via H_2O_2) can minimize cellular apoptosis, exposure which lasts for more than 48 hours is often detrimental [30]. Research has also demonstrated that both the activation and expansion of CPCs *in vivo* is specific to their extracellular environment. For example, fibronectin is a critical extracellular matrix protein responsible for the activation of c-Kit+ CPCs following MI. In an inducible fibronectin knockdown mouse model, c-Kit+ CPCs failed to expand *in vivo* following MI which coincided with significant functional deterioration [31]. Collagen dominates the extracellular matrix composition of the 4 week infarct ECM and therefore fibronectin comprises a smaller fraction of the infarct ECM relative to the healthy ECM [16]. A decrease in fibronectin within the chronic model likely contributed to the reduced proliferative potential of c-Kit+ CPCs relative to the healthy model. The increased expression of the alpha2 integrin could suggest an increase in adhesion to collagen-specific ligands relative to the healthy environment [32]. Moreover, because integrin-mediated signaling influences several cellular signaling pathways including differentiation, apoptosis, and proliferation [33], it is likely that the infarct ECM negatively impacts cell engraftment and proliferation. However, a more thorough investigation into integrin signaling pathways is needed to identify the specific mechanisms responsible for the decreased adhesion and proliferation within the infarct environment.

In our model system, the potential for cardiac differentiation was minimal and difficult to promote with the application of an implantation strategy. The cardiomyogenic potential of CPCs has been heavily debated and while several researchers have demonstrated the ability to direct cardiac differentiation *in vitro* with the manipulation of various culture conditions [34], our model system supports previous reports that signaling moieties within the native myocardial environment do not induce spontaneous differentiation of CPCs [2]. Moreover, our results highlight the variability which arises in the isolation and expansion of CPCs and this variability is likely attributable to the heterogeneity in CPC activation following injury. Similar to previous reports [35–37], the cardiomyogenic potential of CPCs appears to be significantly regulated by their ISL-1 expression. Previous work has demonstrated that the delivery of recombinant Isl-1 protein increases the percentage of functional cardiomyocytes derived from human embryonic stem cells and Isl-1+ cells contribute to a significant percentage of resident cells in the heart as demonstrated in an Isl-1 knockout mouse model, in which animals lack an outflow tract, right ventricle and regions of the atria [37]. While in humans it has been debated whether a subpopulation of CPC progenitors which concurrently express Isl-1 and c-Kit exists [38], other researchers have isolated subpopulations of c-Kit+ CPCs which express Isl-1 from specific animal models including sheep and rats [39]. Given the strong correlation between ISL-1 expression and TNNT2 expression observed in the

Author Manuscript Author Manuscript Author Manuscript Author Manuscript

absence of stem maintenance media, our research supports the hypothesis that the development of strategies which stimulate and/or promote ISL-1 expression by CPCs is likely to maximize their cardiac differentiation potential *in vivo*. Despite the robust expression of TNNT2 by line 2, it is important to emphasize the immaturity of this progenitor phenotype which appears both morphologically and functionally dissimilar to a native cardiomyocyte. Therefore, it remains to be seen whether this cell type has any true potential for functional repair via directed cardiac differentiation to functional cardiomyocytes *in vivo*.

In addition to the initial degree of ISL-1 expression in the isolated population, stiffness and cytokines also influenced the expression of TNNT2. Previous differentiation protocols have highlighted the importance of substrate stiffness in directing the cardiac differentiation of pluripotent stem cells (PSCs), with strong correlations existing between substrate rigidity and the percentage of TnT+ cells [40]. Engler et al demonstrated that MSCs cultured on gels of an intermediate stiffness (8–17 kPa) had the greatest expression of the muscle transcription factor MyoD, while neurogenic and osteogenic differentiation was more robust on the softer and more rigid gels, respectively [22]. Work has also demonstrated that increased matrix stiffness impedes functional maturation of immature cardiomyocytes [41] as well as minimizes the electrical excitability of myocytes [42] and the forces generated during spontaneous contraction [43]. Therefore, the increased stiffness of the myocardial scar may promote the expression of early cardiac differentiation markers, but impede the functional maturation of a CPC, which would be necessary for the restoration of contractility within the injured myocardial environment.

The negative correlation between inflammatory mediators and TNNT2 expression is likely attributable to both TGF-β-induced proliferation [44] and FGF-maintained stemness [45], which together inhibit the percentage of cells differentiating towards either a cardiac or vascular lineage. This hypothesis is further supported by the negative correlations which exist between cytokine presence and all five of the genes explored in the multivariate linear regression analysis. GATA4 expression was minimally impacted by the four infarct variables assessed in this study, including cytokine presence. The transcription factor is robustly expressed by both immature CPCs and differentiated cardiomyocytes and therefore, it is difficult to make conclusions regarding GATA4 expression and the differentiation potential of c-Kit+ CPCs.

Unlike cardiac differentiation potential, the robust expression of both VWF and TAGLN suggests that the native environment is conducive to vascular differentiation of resident CPCs [46]. Unfortunately, this differentiation potential is significantly abrogated by the infarct environment. Although increasing substrate stiffness promoted VWF expression, this response was negated within the model system most likely due to the presence of fibrotic mediators as well as the decreased oxygen tension. Previous research has demonstrated that prolonged exposure to oxidative stress can inhibit CPC expression of both smooth muscle and endothelial genes [30]. Despite poor adhesion, proliferation and differentiation potential, the infarct model promoted the expression of two critical growth factors, HGF and VEGF, which enhance cell survival and promote angiogenesis *in vivo*. Paracrine signaling is considered to be one of the predominant mechanisms by which stem cell therapy promotes

Author Manuscript Author Manuscript Author Manuscript Author Manuscript

functional restoration following MI. In particular, the injection of HGF one day following MI decreases cellular apoptosis via the activation of the PI3-kinase/Akt pathway, which results in enhanced systolic function 4 weeks following injury [47]. We have previously demonstrated that 4 week infarct matrix promotes the expression and secretion of HGF by MSCs as compared to standard tissue culture plastic and healthy matrix [16]. Because the HGF receptor is influenced by integrin-mediated signaling [48] and the secretion of HGF is responsible for anti-fibrotic signaling [49], it is likely that the increased collagen density of the 4 week ECM enhances the expression of this growth factor within the infarct model system.

The model not only highlighted differences in cellular adhesion, expansion, differentiation and growth factor signaling across the two environments, but also demonstrated significant discrepancies across cell lines. Several infarct variables regulated cardiac differentiation potential, but the initial degree of ISL-1 expression in the isolate was the strongest predictor of both GATA4 and TNNT2 expression and this stem marker varied significantly in lines 2, 3 and 5. Despite isolating all cellular populations one week post-MI and sorting for the c-Kit cell surface antigen, the populations were heterogeneous not only following isolation, but also with their response following seeding in the infarct model microenvironment as demonstrated by the variability in the adhesion, expansion and gene expression data sets. Stratifying the data by line identified stronger correlations across infarct variables and differentiation markers (Table 3) and more importantly, by excluding line 5 from the regression analysis entirely (Supplemental Table 1), the goodness of fit described by the adjusted R^2 value increased. Inter-patient heterogeneity in stem cell clones has been well documented in both PSCs and MSCs. For example, hematopoietic-differentiation potential of induced PSCs varied more significantly across patient derived clones than across cells generated from the same patient [50]. In addition, the expression of the pro-angiogenic guidance molecule, SLIT3 by MSCs varied from clone to clone and regulated the vascularization potential of the cells *in vivo* [51]. Therefore, identifying the optimal strategy for regenerating infarcted myocardium will likely be tightly regulated by the population of CPCs isolated from a specific patient. The model described demonstrates significant potential for determining the most beneficial approach to CPC implantation at the patient-specific level.

While the model system enables a simple and potentially accurate prediction of cell fate *in vivo*, several key variables not included within the current model likely regulate cellular adhesion, viability and differentiation. Increasing the complexity of the model system by transitioning to a three-dimensional system, including additional cell types such as cardiac fibroblasts, incorporating physical stimulation by culturing the model environments within bioreactors that can elicit both electrical and mechanical stimulation as well as the inclusion of additional cytokines and inflammatory mediators (MMPs) will likely improve the predictive capacity of the current system. While these manipulations may reduce the ease and reproducibility of cell culture and fate assessment, they are likely critical factors regulating cell fate following implantation. However, even by increasing the complexity of the model system, it is still challenging to fully recapitulate the *in vivo* environment within an *in vitro* cell culture platform. Therefore, the current model may serve as a foundation for

Author Manuscript Author Manuscript Author Manuscript Author Manuscript

the development of future model systems, which will be valuable for the development of clinical strategies, which promote the efficacy of cell therapy. Also, decellularization of the infarcted hearts required the use of a strong detergent (1% SDS). It has been suggested that strong detergents such as SDS remove several critical biofactors known to influence cell fate including proteoglycans and glycosaminoglycans [52]. Therefore, the evaluation of additional detergents for the decellularization process may increase the validity of the model system by maintaining the robust nature of binding motifs present within the native myocardial environment. In addition, our method of solubilization of the ECM may reduce the accuracy of the model system because it no longer provides structural cues to the cells and soluble ECM fragments have demonstrated the potential to be proinflammatory [53]. It is important to note, however, these ECM fragments would likely be present in the infarct microenvironment. Development of alternative methods for incorporating whole ECM in a nondigested form will likely improve the model system. Furthermore, the regression analysis assumes linear relationships between each of the independent variables and genes of interest. These are most likely over simplified relationships, which fail to describe the complex interactions that occur *in vivo*. In order to improve the predictive power of the test, additional non-linear relationships should be examined.

Conclusion

Overall, our results highlight the importance in characterizing an individual's population of CPCs prior to implantation in order to understand their therapeutic efficacy within the inhospitable myocardial scar. While the environment is generally detrimental to vascular and cardiac differentiation, the enhancement of paracrine signaling within the infarct model suggests that the implanted cells may function primarily through pro-survival and pro-angiogenic paracrine signaling with native cells to elicit the significant functional repair which has been observed clinically. Finally, the significant correlations which exist between ISL-1 expression and CPC cardiomyogenic potential suggests that screening the cells for this marker or eliciting its expression *ex vivo* may enhance therapeutic efficacy *in vivo*. Further development and application of this model system will likely promote functional recovery achieved via cell therapy for the treatment of MI and prevention of HF.

Supplementary Material

Refer to Web version on PubMed Central for supplementary material.

Acknowledgements

This work was funded by the American Heart Association (Grant No. 14PRE19960001 to K.E.S.) and the National Institutes of Health, National Heart, Lung and Blood Institute (Grant No. R00HL093358 to L.D.B).

Literature Cited

1. Go AS, Mozaffarian D, Roger VL, Benjamin EJ, Berry JD, Borden WB, et al. Heart Disease and Stroke Statistics—2013 Update: A Report From the American Heart Association. Circulation. 2013; 127:e6–e245. [PubMed: 23239837]
2. van Berlo JH, Kanisicak O, Maillet M, Vagnozzi RJ, Karch J, Lin S-CJ, et al. c-kit+ cells minimally contribute cardiomyocytes to the heart. Nature. 2014; 509:337–341. [PubMed: 24805242]

Author Manuscript Author Manuscript Author Manuscript Author Manuscript

3. Jesty SA, Steffey MA, Lee FK, Breitbach M, Hesse M, Reining S, et al. c-kit+ precursors support postinfarction myogenesis in the neonatal, but not adult, heart. Proc Natl Acad Sci U S A. 2012; 109:13380–13385. [PubMed: 22847442]
4. Malliaras K, Makkar RR, Smith RR, Cheng K, Wu E, Bonow RO, et al. Intracoronary cardiosphere derived cells after myocardial infarction: evidence of therapeutic regeneration in the final 1-year results of the CADUCEUS trial (CArdiosphere-Derived aUtologous stem CElls to reverse ventricular dySfunction). Journal of the American College of Cardiology. 2014; 63:110–122. [PubMed: 24036024]
5. Tallini YN, Greene KS, Craven M, Spealman A, Breitbach M, Smith J, et al. c-kit expression identifies cardiovascular precursors in the neonatal heart. Proceedings of the National Academy of Sciences. 2009
6. Huang C, Gu H, Yu Q, Manukyan MC, Poynter JA, Wang M. Sca-1+ cardiac stem cells mediate acute cardioprotection via paracrine factor SDF-1 following myocardial ischemia/reperfusion. PloS one. 2011; 6:e29246. [PubMed: 22195033]
7. Gray WD, French KM, Ghosh-Choudhary SK, Maxwell JT, Brown ME, Platt MO, et al. Identification of Therapeutic Covariant microRNA Clusters in Hypoxia Treated Cardiac Progenitor Cell Exosomes using Systems Biology. Circulation research. 2014
8. Hu S, Huang M, Nguyen PK, Gong Y, Li Z, Jia F, et al. Novel microRNA prosurvival cocktail for improving engraftment and function of cardiac progenitor cell transplantation. Circulation. 2011; 124:S27–S34. [PubMed: 21911815]
9. St John Sutton M, Pfeffer MA, Moye L, Plappert T, Rouleau JL, Lamas G, et al. Cardiovascular death and left ventricular remodeling two years after myocardial infarction: baseline predictors and impact of long-term use of captopril: information from the Survival and Ventricular Enlargement (SAVE) trial. Circulation. 1997; 96:3294–3299. [PubMed: 9396419]
10. Sandstedt J, Jonsson M, Dellgren G, Lindahl A, Jeppsson A, Asp J. Human C-kit+CD45- cardiac stem cells are heterogeneous and display both cardiac and endothelial commitment by single-cell qPCR analysis. Biochem Biophys Res Commun. 2014; 443:234–238. [PubMed: 24309111]
11. French KM, Boopathy AV, DeQuach JA, Chingozha L, Lu H, Christman KL, et al. A naturally derived cardiac extracellular matrix enhances cardiac progenitor cell behavior in vitro. Acta Biomaterialia. 2012; 8:4357–4364. [PubMed: 22842035]
12. Williams C, Budina E, Stoppel WL, Sullivan KE, Emani S, Emani SM, et al. Cardiac extracellular matrix-fibrin hybrid scaffolds with tunable properties for cardiovascular tissue engineering. Acta Biomater. 2014
13. Yan F, Yao Y, Chen L, Li Y, Sheng Z, Ma G. Hypoxic Preconditioning Improves Survival of Cardiac Progenitor Cells: Role of Stromal Cell Derived Factor-1α–CXCR4 Axis. PloS one. 2012; 7:e37948. [PubMed: 22815687]
14. Takehara N, Tsutsumi Y, Tateishi K, Ogata T, Tanaka H, Ueyama T, et al. Controlled delivery of basic fibroblast growth factor promotes human cardiosphere-derived cell engraftment to enhance cardiac repair for chronic myocardial infarction. Journal of the American College of Cardiology. 2008; 52:1858–1865. [PubMed: 19038683]
15. Goumans M-J, de Boer TP, Smits AM, van Laake LW, van Vliet P, Metz CHG, et al. TGF-β1 induces efficient differentiation of human cardiomyocyte progenitor cells into functional cardiomyocytes in vitro. Stem Cell Research. 2008; 1:138–149. [PubMed: 19383394]
16. Sullivan KE, Quinn KP, Tang KM, Georgakoudi I, Black LD 3rd, et al. Extracellular matrix remodeling following myocardial infarction influences the therapeutic potential of mesenchymal stem cells. Stem Cell Res Ther. 2014; 5:14. [PubMed: 24460869]
17. Yuan Ye K, Sullivan KE, Black LD. Encapsulation of cardiomyocytes in a fibrin hydrogel for cardiac tissue engineering. J Vis Exp. 2011
18. DeQuach JA, Mezzano V, Miglani A, Lange S, Keller GM, Sheikh F, et al. Simple and High Yielding Method for Preparing Tissue Specific Extracellular Matrix Coatings for Cell Culture. PloS one. 2010; 5:e13039. [PubMed: 20885963]
19. Berry MF, Engler AJ, Woo YJ, Pirolli TJ, Bish LT, Jayasankar V, et al. Mesenchymal stem cell injection after myocardial infarction improves myocardial compliance. American journal of physiology Heart and circulatory physiology. 2006; 290:H2196–H2203. [PubMed: 16473959]

Author Manuscript Author Manuscript Author Manuscript Author Manuscript

20. Pelham RJ, Wang Y-l. Cell locomotion and focal adhesions are regulated by substrate flexibility. Proceedings of the National Academy of Sciences of the United States of America. 1997; 94:13661–13665. [PubMed: 9391082]
21. Roy S, Khanna S, Wallace WA, Lappalainen J, Rink C, Cardounel AJ, et al. Characterization of perceived hyperoxia in isolated primary cardiac fibroblasts and in the reoxygenated heart. The Journal of biological chemistry. 2003; 278:47129–47135. [PubMed: 12952964]
22. Engler AJ, Sen S, Sweeney HL, Discher DE. Matrix elasticity directs stem cell lineage specification. Cell. 2006; 126:677–689. [PubMed: 16923388]
23. Mendler N, Schuchhardt S, Sebening F. Measurement of intramyocardial oxygen tension during cardiac surgery in man. Research in experimental medicine Zeitschrift fur die gesamte experimentelle Medizin einschliesslich experimenteller Chirurgie. 1973; 159:231–238. [PubMed: 4687013]
24. Iwabu A, Murakami T, Kusachi S, Nakamura K, Takemoto S, Komatsubara I, et al. Concomitant expression of heparin-binding epidermal growth factor-like growth factor mRNA and basic fibroblast growth factor mRNA in myocardial infarction in rats. Basic research in cardiology. 2002; 97:214–222. [PubMed: 12061391]
25. Deten A, Holzl A, Leicht M, Barth W, Zimmer HG. Changes in extracellular matrix and in transforming growth factor beta isoforms after coronary artery ligation in rats. Journal of molecular and cellular cardiology. 2001; 33:1191–1207. [PubMed: 11444923]
26. Rowlands DJ, Islam MN, Das SR, Huertas A, Quadri SK, Horiuchi K, et al. Activation of TNFR1 ectodomain shedding by mitochondrial Ca2+ determines the severity of inflammation in mouse lung microvessels. The Journal of clinical investigation. 2011; 121:1986–1999. [PubMed: 21519143]
27. Fomovsky GM, Holmes JW. Evolution of scar structure, mechanics, and ventricular function after myocardial infarction in the rat. American journal of physiology Heart and circulatory physiology. 2010; 298:H221–H228. [PubMed: 19897714]
28. Jugdutt BI, Joljart MJ, Khan MI. Rate of collagen deposition during healing and ventricular remodeling after myocardial infarction in rat and dog models. Circulation. 1996; 94:94–101. [PubMed: 8964124]
29. van der Laan AM, Nahrendorf M, Piek JJ. Healing and adverse remodelling after acute myocardial infarction: role of the cellular immune response. Heart. 2012; 98:1384–1390. [PubMed: 22904145]
30. Pendergrass KD, Boopathy AV, Seshadri G, Maiellaro-Rafferty K, Che PL, Brown ME, et al. Acute preconditioning of cardiac progenitor cells with hydrogen peroxide enhances angiogenic pathways following ischemia-reperfusion injury. Stem Cells Dev. 2013; 22:2414–2424. [PubMed: 23544670]
31. Konstandin MH, Toko H, Gastelum GM, Quijada P, De La Torre A, Quintana M, et al. Fibronectin is essential for reparative cardiac progenitor cell response after myocardial infarction. Circulation research. 2013; 113:115–125. [PubMed: 23652800]
32. Knight CG, Morton LF, Peachey AR, Tuckwell DS, Farndale RW, Barnes MJ. The collagen-binding A-domains of integrins alpha(1)beta(1) and alpha(2)beta(1) recognize the same specific amino acid sequence, GFOGER, in native (triple-helical) collagens. J Biol Chem. 2000; 275:35–40. [PubMed: 10617582]
33. Bowers SL, Banerjee I, Baudino TA. The extracellular matrix: at the center of it all. Journal of molecular and cellular cardiology. 2010; 48:474–482. [PubMed: 19729019]
34. Smith AJ, Lewis FC, Aquila I, Waring CD, Nocera A, Agosti V, et al. Isolation and characterization of resident endogenous c-Kit+ cardiac stem cells from the adult mouse and rat heart. Nat Protocols. 2014; 9:1662–1681. [PubMed: 24945383]
35. Bu L, Jiang X, Martin-Puig S, Caron L, Zhu S, Shao Y, et al. Human ISL1 heart progenitors generate diverse multipotent cardiovascular cell lineages. Nature. 2009; 460:113–117. [PubMed: 19571884]
36. Cohen ED, Wang Z, Lepore JJ, Lu MM, Taketo MM, Epstein DJ, et al. Wnt/β-catenin signaling promotes expansion of Isl-1–positive cardiac progenitor cells through regulation of FGF signaling. Journal of Clinical Investigation. 2007; 117:1794–1804. [PubMed: 17607356]

Author Manuscript Author Manuscript Author Manuscript Author Manuscript

37. Cai CL, Liang X, Shi Y, Chu PH, Pfaff SL, Chen J, et al. Isl1 identifies a cardiac progenitor population that proliferates prior to differentiation and contributes a majority of cells to the heart. Developmental cell. 2003; 5:877–889. [PubMed: 14667410]
38. Serradifalco C, Catanese P, Rizzuto L, Cappello F, Puleio R, Barresi V, et al. Embryonic and foetal Islet-1 positive cells in human hearts are also positive to c-Kit. European journal of histochemistry : EJH. 2011; 55:e41. [PubMed: 22297447]
39. Hou X, Appleby N, Fuentes T, Longo LD, Bailey LL, Hasaniya N, et al. Isolation, Characterization, and Spatial Distribution of Cardiac Progenitor Cells in the Sheep Heart. Journal of clinical & experimental cardiology. 2012:S6.
40. Arshi A, Nakashima Y, Nakano H, Eaimkhong S, Evseenko D, Reed J, et al. Rigid microenvironments promote cardiac differentiation of mouse and human embryonic stem cells. Science and technology of advanced materials. 2013; 14:025003. [PubMed: 24311969]
41. Jacot JG, McCulloch AD, Omens JH. Substrate Stiffness Affects the Functional Maturation of Neonatal Rat Ventricular Myocytes. Biophysical Journal. 2008; 95:3479–3487. [PubMed: 18586852]
42. Bhana B, Iyer RK, Chen WLK, Zhao R, Sider KL, Likhitpanichkul M, et al. Influence of substrate stiffness on the phenotype of heart cells. Biotechnol Bioeng. 2010; 105:1148–1160. [PubMed: 20014437]
43. Shapira-Schweitzer K, Seliktar D. Matrix stiffness affects spontaneous contraction of cardiomyocytes cultured within a PEGylated fibrinogen biomaterial. Acta Biomater. 2007; 3:33–41. [PubMed: 17098488]
44. Stewart A, Guan H, Yang K. BMP-3 promotes mesenchymal stem cell proliferation through the TGF-beta/activin signaling pathway. Journal of cellular physiology. 2010; 223:658–666. [PubMed: 20143330]
45. Gotoh N. Control of stemness by fibroblast growth factor signaling in stem cells and cancer stem cells. Current stem cell research & therapy. 2009; 4:9–15. [PubMed: 19149625]
46. Tillmanns J, Rota M, Hosoda T, Misao Y, Esposito G, Gonzalez A, et al. Formation of large coronary arteries by cardiac progenitor cells. Proceedings of the National Academy of Sciences. 2008; 105:1668–1673.
47. Wang Y, Ahmad N, Wani MA, Ashraf M. Hepatocyte growth factor prevents ventricular remodeling and dysfunction in mice via Akt pathway and angiogenesis. Journal of molecular and cellular cardiology. 2004; 37:1041–1052. [PubMed: 15522281]
48. Chan PC, Chen SY, Chen CH, Chen HC. Crosstalk between hepatocyte growth factor and integrin signaling pathways. Journal of biomedical science. 2006; 13:215–2123. [PubMed: 16496226]
49. Schievenbusch S, Strack I, Scheffler M, Wennhold K, Maurer J, Nischt R, et al. Profiling of antifibrotic signaling by hepatocyte growth factor in renal fibroblasts. Biochem Biophys Res Commun. 2009; 385:55–61. [PubMed: 19426716]
50. Mills JA, Wang K, Paluru P, Ying L, Lu L, Galvao AM, et al. Clonal genetic and hematopoietic heterogeneity among human-induced pluripotent stem cell lines. Blood. 2013; 122:2047–2051. [PubMed: 23940280]
51. Paul JD, Coulombe KL, Toth PT, Zhang Y, Marsboom G, Bindokas VP, et al. SLIT3-ROBO4 activation promotes vascular network formation in human engineered tissue and angiogenesis in vivo. Journal of molecular and cellular cardiology. 2013; 64:124–131. [PubMed: 24090675]
52. Mendoza-Novelo B, Avila EE, Cauich-Rodríguez JV, Jorge-Herrero E, Rojo FJ, Guinea GV, et al. Decellularization of pericardial tissue and its impact on tensile viscoelasticity and glycosaminoglycan content. Acta Biomaterialia. 2011; 7:1241–1248. [PubMed: 21094703]
53. Adair-Kirk TL, Senior RM. Fragments of Extracellular Matrix as Mediators of Inflammation. The international journal of biochemistry & cell biology. 2008; 40:1101–1110. [PubMed: 18243041]

Author Manuscript Author Manuscript Author Manuscript Author Manuscript

Highlights

- Infarct milieu *in vitro* model predicts cell fate and implantation strategy efficacy
- CPCs demonstrate poor engraftment/differentiation potential within infarct model
- Infarct milieu promotes pro-survival/pro-angiogenic growth factor expression
- Model highlights how sensitivity to infarct variables is line-dependent
- Potential for clinical application to identify patient-specific delivery strategy

Author Manuscript Author Manuscript Author Manuscript Author Manuscript

A

	Healthy Model	Infarct Model
ECM	Healthy	4 week
Stiffness	25 kPa	40 kPa
Oxygen	5%	1%
Cytokines	None	TGF-β, bFGF

B

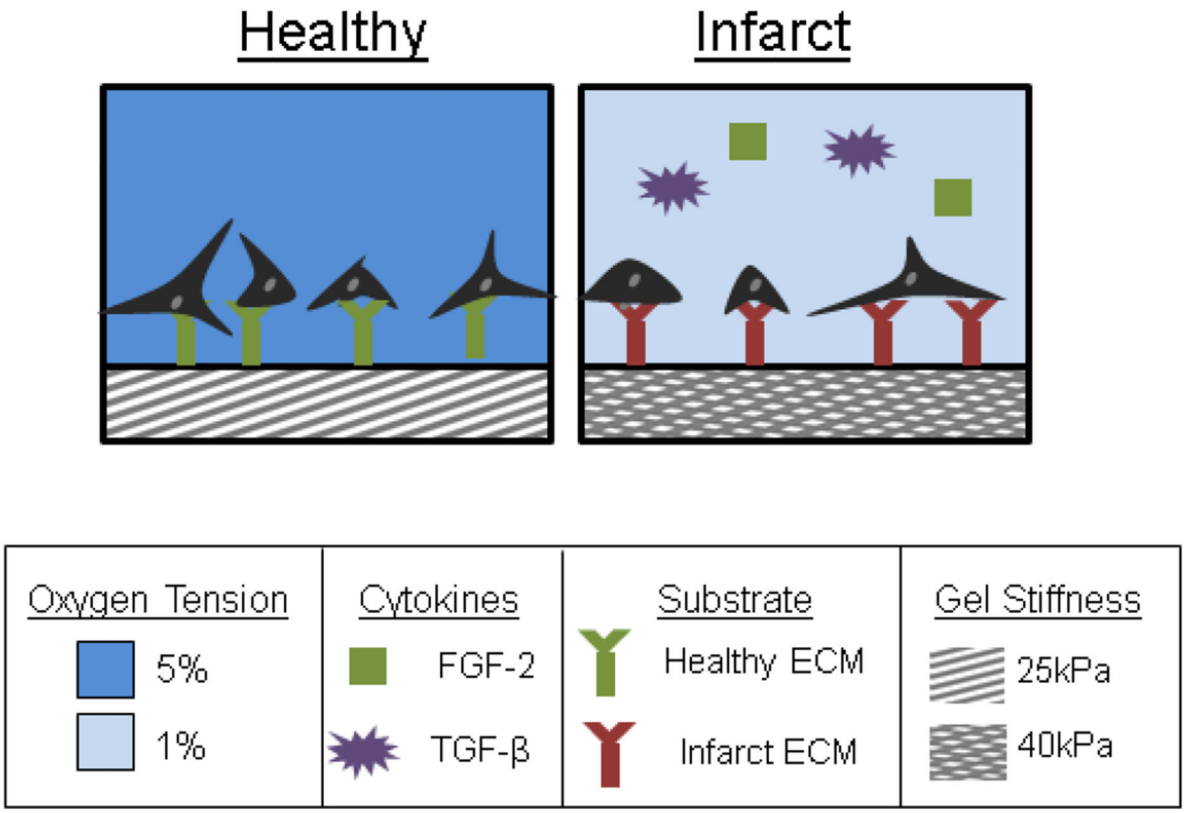

Figure 1.

Development of In Vitro Model of Myocardial Infarction. A. Table describes how each of the four variables (ECM composition, polyacrylamide gel stiffness, oxygen tension and cytokine presence) change as a function of both the healthy and infarct model systems. B. Schematic illustrating the polyacrylamide gel based in vitro model system.

Author Manuscript Author Manuscript Author Manuscript Author Manuscript

A

B

	Stem		Vascular			Cardiac			
	Kit	Isl1	Gata6	Vwf	Kdr	Gata4	Nkx2.5	Tbx5	Tnnt2
Line 1	*	*	***	*	NE	**	*	*	*
Line 2	*	*	***	*	NE	**	*	NE	*
Line 3	*	*	***	*	*	**	*	*	*
Line 4	*	NE	***	*	*	***	NE	*	*
Line 5	*	NE	*	*	*	**	NE	*	*
Line 6	*	NE	****	*	NE	***	NE	**	***

NE: Not expressed
*: 5 ≤ ΔCt
**: 3 ≤ ΔCt < 5
***: 1 ≤ ΔCt < 3
****: -1 ≤ ΔCt < 1

C

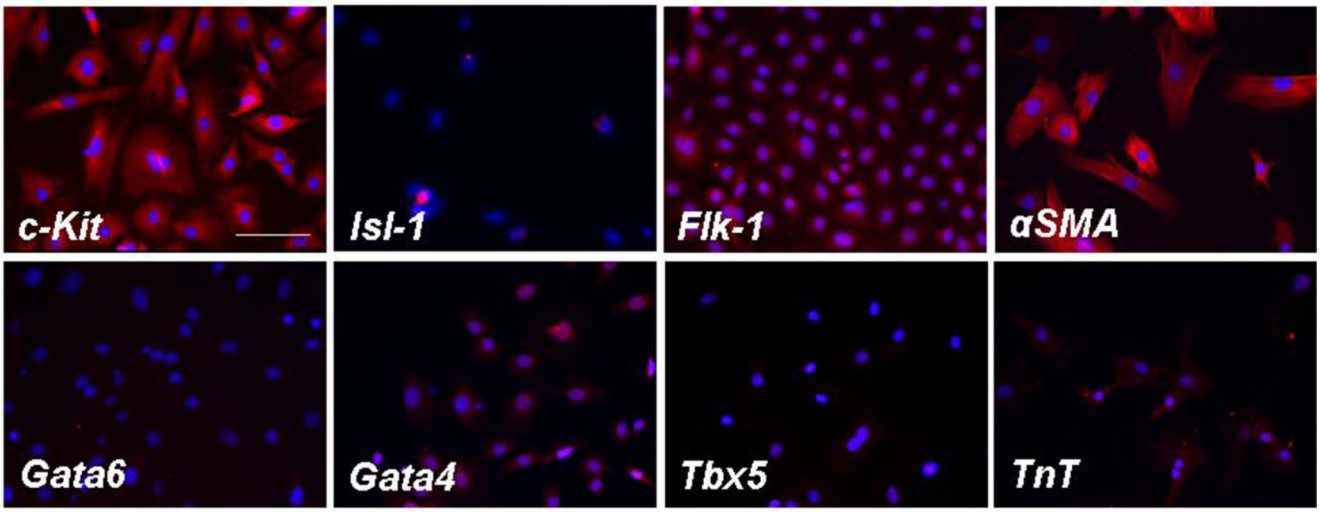

Figure 2.

Isolation and Characterization of c-Kit+ CPCs. A. 1 week following induction of MI (suture which ligated coronary artery highlighted by arrow), c-Kit+ CPCs are isolated via a collagenase type II digestion followed by MACs sorting for c-Kit antibody. B. 6 lines of cells were isolated from 6 distinct infarcted hearts and heterogeneity was characterized via qPCR at passages 2 or 3 following culture in stem maintenance media. C. Histological assessment of Line 5 demonstrates that cells maintain a stem phenotype in culture as evidenced by c-Kit expression. However, this line of cells does not positively express Isl-1, Gata6, Tbx5 of TnT. However, the cells still possess characteristics of cardiac and vascular progenitors by their positive expression of Flk-1, aSMA, and Gata4. Scale bar is 100 μm. All images taken at 20×.

Author Manuscript
Author Manuscript
Author Manuscript
Author Manuscript

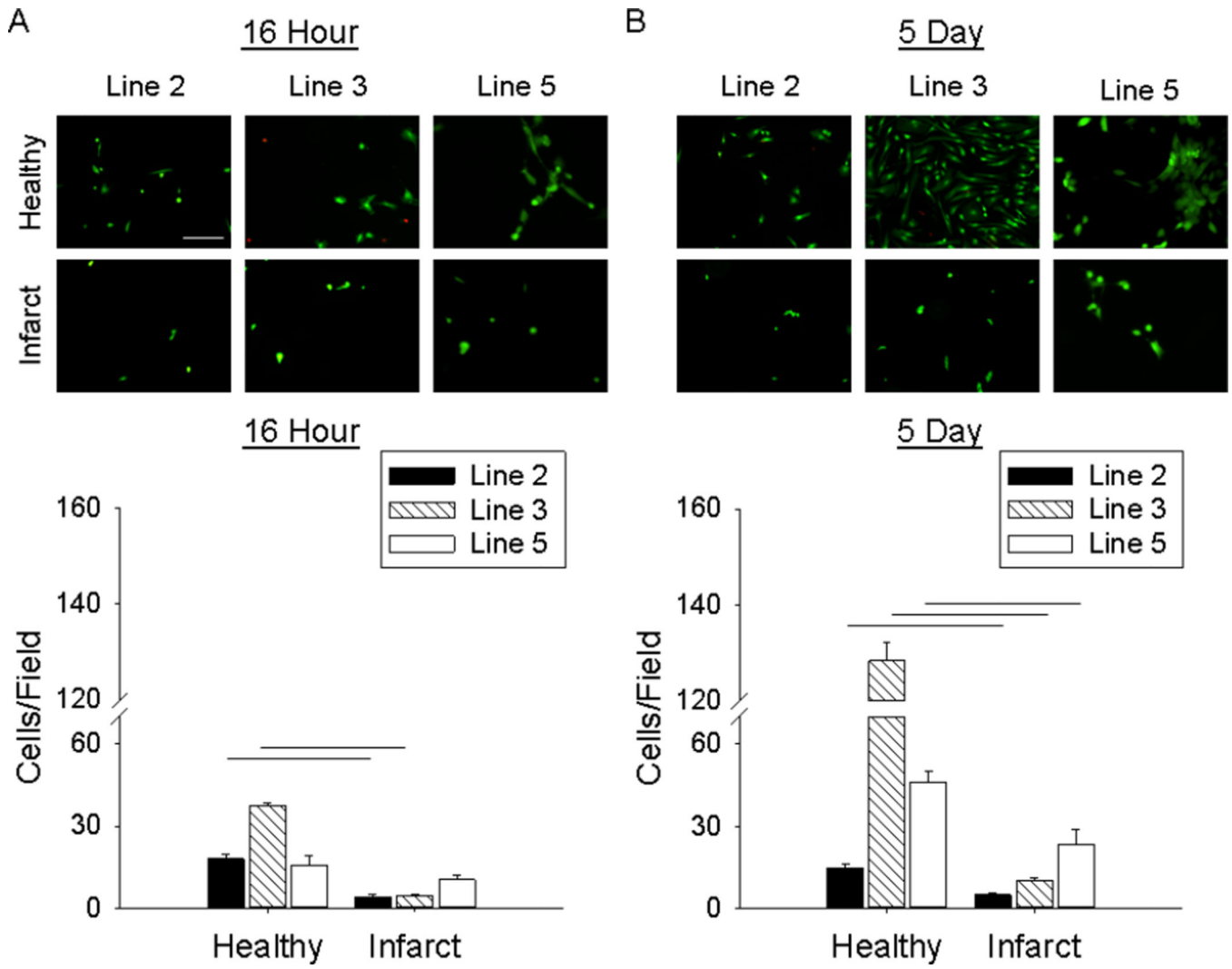

Figure 3.

Infarct Model Impedes Cellular Adhesion and Proliferation. A. At 16 hours post-seeding, qualitative image assessment of Live/Dead stain demonstrates that the healthy model significantly promotes cell adhesion. Quantitative image analysis demonstrates a significantly greater number of cells in the healthy model for Lines 2 and 3 at 16 hours post-seeding. B. At 5 days and for all three lines, the cells proliferate much more rapidly in the healthy environment relative to the infarct model. All images are taken with a 20× objective and scale bar is 100 μm. Lines indicate significance with a $p<0.05$.

Author Manuscript Author Manuscript Author Manuscript Author Manuscript

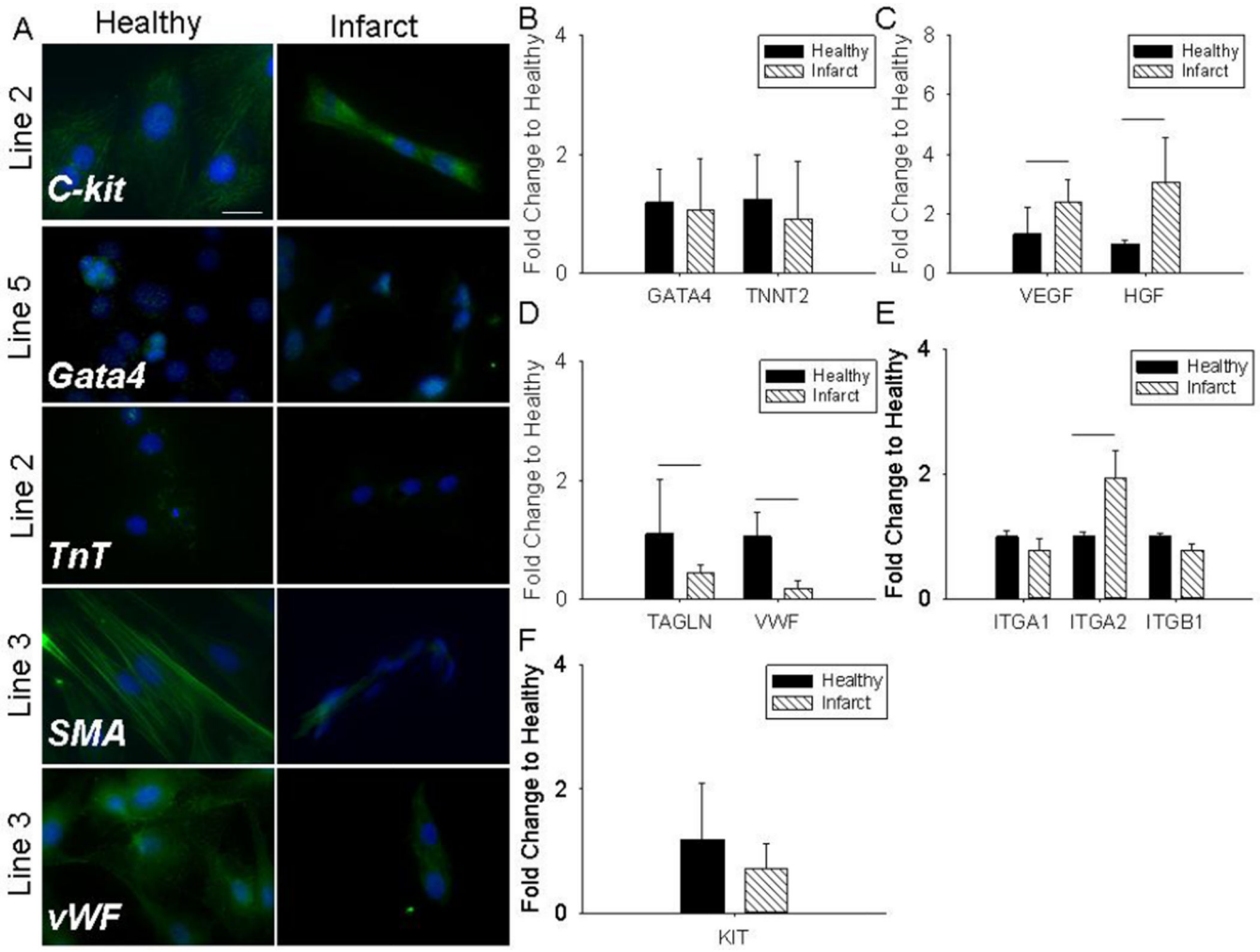

Figure 4.

Assessing Regenerative Potential of c-Kit+ CPCs within Model System. A. Histological assessment demonstrates decreased differentiation potential within infarct environment. In particular, vascular markers (α-SMA and vWF) appear absent within the infarct model, but robust within the healthy model. Images taken at 60× oil immersion and scale bar is 25 μm. B. Cardiac differentiation potential assessed through qPCR does not change as a function of the infarct environment. C. Gene expression of pro-survival (HGF) and pro-angiogenic (VEGF) growth factors increases significantly within the infarct microenvironment relative to the healthy ($p=0.01$ and 0.017, respectively). D. TAGLN and VWF gene expression significantly decreases within the infarct model ($p=0.002$ and $p<0.001$, respectively). E. Integrin α2 gene expression increases significantly within the infarct model ($p=0.025$). F. KIT expression is not significantly altered as a function of the infarct microenvironment. All gene expression is presented as mean +/− SD.

Author Manuscript
Author Manuscript
Author Manuscript
Author Manuscript

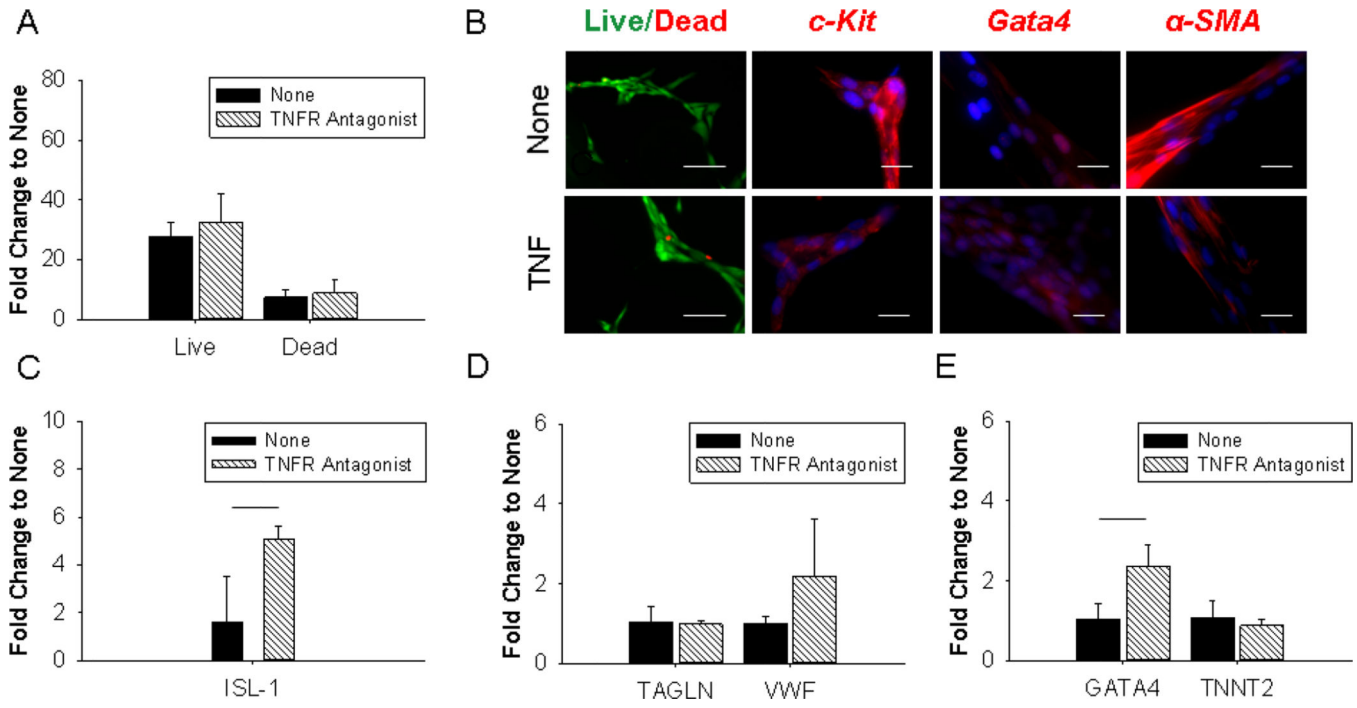

Figure 5.

Implantation Strategy Influences Differentiation Potential of c-Kit+ CPCs. A. Cell profiler analysis of live/dead staining 5 days post seeding demonstrates no significant change in the number of live cells/field (mean +/− SE) following treatment with aTNFα receptor antagonist.. B. 5 days post-seeding, live/dead staining of c-Kit+ CPCs seeded in the infarct model in the absence of an implantation strategy (None) and in the presence of a TNFα receptor antagonist (TNFR Antagonist) demonstrate similar levels of cell adhesion and viability (scale bar represents 100 μm). Histological staining demonstrates variable stem marker, cardiac and vascular differentiation potential across the two implantation strategies. Images taken at 60× oil immersion and scale bar represents 25 μm. B. C. The cardiac progenitor phenotype is enhanced with the implantation strategy as compared to no treatment as demonstrated by an increase in Isl-1 gene expression. Data presented as mean +/− SD and p=0.041. D. VWF and TAGLN gene expression do not change significantly with the delivery of a TNFα receptor antagonist. E. Gata4 gene expression is enhanced when cells are delivered with a TNFα receptor antagonist, but TNNT2 expression is unaltered. Data presented as mean +/− SD and p=0.04.

Author Manuscript Author Manuscript Author Manuscript Author Manuscript

Table 1

Normalized values for each independent variable modeled within the infarct system are defined. These normalized values were applied during multiple linear regression analysis.

Independent Variables	Independent Variable Normalization for Regression Analysis						
Line (ISL-1 Expression)	Line 5		Line 3			Line 2	
	0		0.5			1	
Composition (Collagen I Density)	0 μg/cm^2	1 μg/cm^2	2 μg/cm^2 (Healthy ECM)	2.5 μg/cm^2	4 μg/cm^2 (Infarct ECM)	5 μg/cm^2	10 μg/cm^2
	0	0.1	0.2	0.25	0.4	0.5	1.0
Stiffness	25 kPa		40 kPa			TCP	
	0.025		0.04			1.0	
Oxygen Tension	1%		5%			20%	
	0.05		0.25			1	
Cytokines	None			FGF/TGFβ			
	0			1			

Author Manuscript Author Manuscript Author Manuscript Author Manuscript

Table 2

Multivariate Regression Analysis.

All Lines		Line		Composition		Stiffness		Oxygen Tension		Cytokines	
	Adj R^2	Coefficient	P-value	Coefficient	P-value	Coefficient	P-value	Coefficient	P-value	Coefficient	P-value
VWF	0.545	0.26	<0.001	0.03	0.705	0.18	0.002	0.15	0.009	-0.18	0.003
TAGLN	0.578	0.2	<0.001	0.14	0.054	0.28	<0.001	0.17	0.005	-0.16	0.002
GATA4	0.876	0.59	<0.001	-0.01	0.759	0.06	0.036	0.07	0.008	-0.04	0.096
TNNT2	0.855	0.57	<0.001	0.08	0.04	0.14	<0.001	0.05	0.148	-0.15	<0.001
ISL1	0.567	0.15	0.023	0.07	0.255	0.24	<0.001	0.22	<0.001	-0.17	<0.001

Adjusted R^2 values describe the goodness of fit of the linear regression model for each gene of interest. The magnitude by which each coefficient regulates gene expression is identified by a color scale. Green identifies a positive interaction, while red indicates an inhibitory interaction. Yellow identifies an intermediate effect. The respective p-value for each coefficient is described in the column to the right of the coefficient. Data from Lines 2, 3 and 5 is included in the regression analysis. A key which describes each independent variable is summarized in Table 1.

Author Manuscript

Author Manuscript

Author Manuscript

Author Manuscript

Table 3

Multivariate Regression Analysis by Line.

	Adj R^2		Composition		Stiffness		Oxygen Tension		Cytokines	
	Line 2	Line 3	Line 2	Line 3	Line 2	Line 3	Line 2	Line 3	Line 2	Line3
VWF	0.727	0.571	-0.065	0.053	0.216*	0.192*	0.309**	0.124	-0.178*	-0.242**
TAGLN	0.734	0.691	0.051	0.105	0.27**	0.283*	0.27**	0.187*	-0.111*	-0.276**
GATA4	0.655	0.676	0.031	0.006	0.105*	0.109**	0.132**	0.038	-0.035	-0.061*
TNNT2	0.887	0.498	0.034	0.106*	0.101**	0.182**	0.151**	-0.018	-0.324**	-0.06
ISL1	0.71	0.472	0.005	0.143	0.143*	0.3*	0.406**	0.025	-0.164**	-0.173*

Adjusted R^2 values describe the goodness of fit of the linear regression model for Lines 2 and 3. The magnitude by which each coefficient regulates gene expression is identified by a color scale. Green identifies a positive interaction, while red indicates an inhibitory interaction. Yellow identifies an intermediate effect. The respective p-value for each coefficient is indicated by an asterisk. ($p<0.05$ is indicated by * while $p<0.001$ is indicated by **). A key which describes each independent variable is summarized in Table 1.